

High-Dimensional Cluster Analysis with the Masked EM Algorithm

Shabnam N. Kadir

s.kadir@ucl.ac.uk

UCL Institute of Neurology and UCL Department of Neuroscience, Physiology, and Pharmacology, University College London, London WC1E 6DE, U.K.

Dan F. M. Goodman

Dan_Goodman@meei.harvard.edu

Eaton-Peabody Laboratories, Massachusetts Eye and Ear Infirmary, Department of Otolaryngology and Laryngology, Harvard Medical School, Boston, MA 02114, U.S.A.

Kenneth D. Harris

kenneth.harris@ucl.ac.uk

UCL Institute of Neurology and UCL Department of Neuroscience, Physiology, and Pharmacology, University College London, London WC1E 6DE, U.K.

Cluster analysis faces two problems in high dimensions: the “curse of dimensionality” that can lead to overfitting and poor generalization performance and the sheer time taken for conventional algorithms to process large amounts of high-dimensional data. We describe a solution to these problems, designed for the application of spike sorting for next-generation, high-channel-count neural probes. In this problem, only a small subset of features provides information about the cluster membership of any one data vector, but this informative feature subset is not the same for all data points, rendering classical feature selection ineffective. We introduce a “masked EM” algorithm that allows accurate and time-efficient clustering of up to millions of points in thousands of dimensions. We demonstrate its applicability to synthetic data and to real-world high-channel-count spike sorting data.

1 Introduction

Cluster analysis is a widely used technique for unsupervised classification of data. A popular method for clustering is fitting a mixture of gaussians, often achieved using the expectation-maximization (EM) algorithm (Dempster, Laird, & Rubin, 1977) and variants thereof (Fraley & Raftery,

D.F.M.G. is now with the Department of Electrical and Electronic Engineering, Imperial College London, London U.K.

2002). In high dimensions, however, this method faces two challenges (Bouveyron & Brunet-Saumard, 2012). First is the “curse of dimensionality,” which leads to poor classification, particularly in the presence of a large number of uninformative features; second, for large and high-dimensional data sets, the computational cost of many algorithms can be impractical. This is particularly the case where covariance matrices must be estimated, leading to computations of order $\mathcal{O}(p^2)$, where p is the number of features; furthermore, even a cost of $\mathcal{O}(p)$ can render a clustering method impractical for applications in which large high-dimensional data sets must be analyzed daily. In many cases, however, the dimensionality problem is solvable, at least in principle, as the features sufficient for classification of any particular data point are a small subset of the total available.

A number of approaches have been suggested for the problem of high-dimensional cluster analysis. One approach consists of modifying the generative model underlying the mixture of gaussians fit to enforce low-dimensional models. For example the mixture of factor analyzers (Ghahramani & Hinton, 1996; McLachlan, Peel, & Bean, 2003) models the covariance matrix of each cluster as a low-rank matrix added to a fixed diagonal matrix forming an approximate model of observation noise. This approach can reduce the number of parameters for each cluster from $\mathcal{O}(p^2)$ to $\mathcal{O}(p)$ and may thus provide a substantial improvement in both computational cost and performance. An alternative approach, which offers the opportunity to reduce both the number of parameters and computational cost substantially below $\mathcal{O}(p)$, is feature selection, whereby a small subset of informative features is selected and other noninformative features are discarded (Raftery & Dean, 2006). A limitation of global feature selection methods, however, is that they cannot deal with the case where different data points are defined by different sets of features. One proposed solution to this consists of assigning each cluster a unique distribution of weights over all features, which has been applied to the case of hierarchical clustering (Friedman & Meulman, 2004).

The algorithm described below was developed to solve the problems of high-dimensional cluster analysis for a particular application: spike sorting of neurophysiological recordings using newly developed high-count silicon microelectrodes (Einevoll, Franke, Hagen, Pouzat, & Harris, 2012). Spike sorting is the problem of identifying the firing times of neurons from electric field signatures recorded using multisite microfabricated neural electrodes (Lewicki, 1998). In low-noise systems, such as retinal explants *ex vivo*, it has been possible to decompose the raw recorded signal into a sum of waveforms, each corresponding to a single action potential (Pillow, Shlens, Chichilnisky, & Simoncelli, 2013; Marre et al., 2012; Prentice et al., 2011). For recordings in the living brain, noise levels are considerably higher, and an approach based on cluster analysis is more often taken. In a typical experiment, this will involve clustering millions of data points, each of which reflects a single action potential waveform that could have been produced

by one of many neurons. Historically, neural probes used in vivo have had only a small number of channels (usually four), typically resulting in feature vectors of 12 dimensions, which required sorting into 10 to 15 clusters. Analysis of “ground truth” shows that the data are quite well approximated by a mixture of gaussians with different covariance matrices between clusters (Harris, Henze, Csicsvari, Hirase, & Buzsáki, 2000). Accordingly, in this low-dimensional case, traditional EM-derived algorithms work close to optimally, although specialized rapid implementation software is required to cluster the millions of spikes recorded on a daily basis (Harris, Kadir, & Goodman, 2000–2013). More recent neural probes, however, contain tens to hundreds of channels, spread over large spatial volumes, and probes with thousands are under development. Because different neurons have different spatial locations relative to the electrode array, each action potential is detected on only a small fraction of the total number of channels, but the subset differs between neurons, ruling out a simple global feature selection approach. Furthermore, because spikes produced by simultaneous firing of neurons at different locations must be clustered independently, most features for any one data point are not simply noise, but must be regarded as missing data. Finally, due to the large volumes of data produced by these methods, we require a solution that is capable of clustering millions of data points in reasonably short running time. Although numerous extensions and alternatives to the simple cluster sorting method have been proposed: (Takahashi, Anzai, & Sakurai, 2003; Quian Quiroga, Nadasdy, & Ben-Shaul, 2004; Wood & Black, 2008; Sahani, 1999; Lewicki, 1998; Gasthaus, Wood, Gorur, & Teh, 2008; Calabrese & Paninski, 2011; Ekanadham, Tranchina, & Simoncelli, 2013; Shoham, Fellows, & Normann, 2003; Franke, Natora, Boucsein, Munk, & Obermayer, 2010; Carin et al. 2013), none have been shown to solve the problems created by high-count electrode arrays.

Here we introduce a “masked EM” algorithm to solve the problem of high-dimensional cluster analysis, as found in the spike-sorting context. The algorithm works in two stages. In the first stage, a “mask vector” is computed for each data point via a heuristic algorithm, encoding a weighting of each feature for every data point. This stage may take advantage of domain-specific knowledge, such as the topological constraint that action potentials occupy a spatially contiguous set of recording channels. In the case that the majority of masks can be set to zero, both the number of parameters per cluster and running time can be substantially below $\mathcal{O}(p)$. We note that the masks are assigned to data points rather than clusters and need be computed only once at the start of the algorithm. The second stage consists of cluster analysis. This is implemented using a mixture-of-gaussians EM algorithm, but with every data point replaced by a virtual mixture of the original feature value and the fixed subthreshold noise distribution weighted by the masks. The use of this virtual mixture distribution avoids the splitting of clusters due to arbitrary threshold crossings. At no point is it

Table 1: Mathematical Notation.

| | |
|--|---|
| Dimensions (number of features) | p |
| Data | $x_{n,i}$, point n , feature i |
| Masks | $m_{n,i} \in [0, 1]$ |
| Cluster label | k |
| Total number of clusters | K |
| Mixture weight, cluster mean, covariance | w_k, μ_k, Σ_k |
| Probability density function of the multivariate gaussian distribution | $\phi(\mathbf{x} \mu_k, \Sigma_k)$ |
| Total number of data points | N |
| Number of points for which feature i is masked | $N_i^{\text{mask}} = \{n : m_{n,i} = 0\} $ |
| Noise mean for feature i | v_i |
| Noise variance for feature i | σ_i^2 |
| Virtual features (random variable) | $\tilde{x}_{n,i}$ |
| Mean of virtual feature | $y_{n,i} = \mathbb{E}[\tilde{x}_{n,i}]$ |
| $z_{n,i}$ | $\mathbb{E}[(\tilde{x}_{n,i})^2]$ |
| Variance of virtual feature | $\eta_{n,i} := \text{Var}(\tilde{x}_{n,i})$ |
| Log likelihood of \tilde{x}_n in cluster k | π_{nk} |
| Set of data points assigned to cluster k | \mathcal{C}_k |
| Subset of \mathcal{C}_k for which feature i is fully masked | \mathcal{M}_{ik} |

required to generate samples from the virtual distribution, as expectations over it can be computed analytically.

2 The Masked EM Algorithm

The mathematical notation used in this article can be found in Table 1.

2.1 Stage 1: Mask Generation. The first stage of the algorithm consists of computing a set of mask vectors indicating which features should be used to classify which data points. Specifically, the outcome of this algorithm is a set of vectors \mathbf{m}_n with components, $m_{n,i} \in [0, 1]$. A value of 1 indicates that feature i is to be used in classifying data point \mathbf{x}_n , a value of 0 indicating it is to be ignored, and intermediate values corresponding to partial weighting. We refer to features being used for classification as unmasked and features being ignored as masked (i.e., concealed). Masked features are not simply set to zero, but are ignored by replacing them with a virtual ensemble of points, drawn from a distribution of subthreshold noise.

The use of masks provides two major advantages over a standard mixture of gaussians classification: it overcomes the curse of dimensionality, because assignment of points to classes is no longer overwhelmed by the noise on the large number of masked channels, and it allows the algorithm to run in time proportional to $\mathcal{O}(\text{unmasked features}^2)$ rather than

$\mathcal{O}(\text{features}^2)$. Because a small number of features may be unmasked for each data point, this can allow computational costs substantially below $\mathcal{O}(p)$. The way masks are chosen can depend on the application domain and typically follows a heuristic method. A simple approach that can work in general is to compute masks based on a standard deviation of each feature:

$$m_{n,i} = \begin{cases} 0 & |x_{n,i}| < \alpha SD_i \\ 1 & |x_{n,i}| > \beta SD_i \\ \frac{|x_{n,i}| - \alpha SD_i}{\beta SD_i - \alpha SD_i} & \alpha SD_i < |x_{n,i}| < \beta SD_i \end{cases} \quad (2.1)$$

This strategy smoothly interpolates between a mask of zero for features below a lower threshold and a mask of 1 for features above a higher threshold; such smooth interpolation avoids the artificial creation of discrete clusters when variables cross a fixed boundary. In the case of spike sorting, a slightly more complex procedure is used to derive the masks, which takes advantage of the topological constraint that spikes must be distributed across continuous groups of recording channels (see section 3.2). In practice, we have found that good performance can be obtained for a range of masking parameters, provided the majority of noninformative features have a mask of 0 and that features that are clearly suprathreshold are given a mask of 1 (see section 3.1).

Once the masks have been computed, an additional set of quantities is precomputed before the main EM loop starts. Specifically, the subthreshold noise mean for feature i , v_i , is obtained by taking the mean of feature i whenever that particular feature is masked, that is, $m_{n,i} = 0$, and analogously, the noise variance for feature i , σ_i^2 :

$$v_i := \frac{1}{N_i^{\text{mask}}} \sum_{n:m_{n,i}=0} x_{n,i}, \quad \sigma_i^2 := \frac{1}{N_i^{\text{mask}}} \sum_{n:m_{n,i}=0} (x_{n,i} - v_i)^2,$$

where $N_i^{\text{mask}} = |\{n : m_{n,i} = 0\}|$.

2.2 Stage 2: Clustering. The second stage consists of a maximum-likelihood mixture-of-gaussians fit, with both the E and M steps modified by replacing each data point \mathbf{x}_n with a virtual ensemble of points $\tilde{\mathbf{x}}_n$ distributed as

$$\tilde{x}_{n,i} = \begin{cases} x_{n,i} & \text{prob } m_{n,i} \\ N(v_i, \sigma_i^2) & \text{prob } 1 - m_{n,i}, \end{cases} \quad (2.2)$$

where $m_{n,i} \in [0, 1]$ is the mask vector component associated with $x_{n,i}$ for the n th spike. Intuitively, any feature below a noise threshold is replaced by a virtual ensemble of the entire noise distribution. The noise on each feature will be modeled as independent univariate gaussian distributions $N(v_i, \sigma_i^2)$ for each i , which we shall refer to as the noise distribution for feature i . This is, of course, a simplification, as the noise may be correlated. However, for tractability, ease of implementation, and, as we shall later show, efficacy, this approximation suffices.

The algorithm maximizes the expectation of the usual log likelihood over the virtual distribution:

$$L(w_k, \boldsymbol{\mu}_k, \boldsymbol{\Sigma}_k) := \sum_{n=1}^N \mathbb{E}_{\tilde{\mathbf{x}}} \left[\log \left(\sum_{k=1}^K w_k \frac{\exp(-\frac{1}{2}(\tilde{\mathbf{x}}_n - \boldsymbol{\mu}_k)^T \boldsymbol{\Sigma}_k^{-1}(\tilde{\mathbf{x}}_n - \boldsymbol{\mu}_k))}{(2\pi)^{d/2} \|\boldsymbol{\Sigma}_k\|^{1/2}} \right) \right].$$

The masked EM algorithm therefore acts as if it were passed an ensemble of points, with each data point replaced by an infinite sample, corresponding to different possibilities for the noisy masked variables. This solves the curse of dimensionality by “disenfranchising” each data point’s masked features, disregarding the value that was actually measured and replacing it by a virtual ensemble that is the same in all cases and thus does not contribute to cluster assignment.

Before we run the EM algorithm, we also compute the following quantities, which will greatly speed up computation of the modified M- and E-steps:

$$\begin{aligned} y_{n,i} &:= \mathbb{E}[\tilde{x}_{n,i}] = m_{n,i}x_{n,i} + (1 - m_{n,i})v_i, \\ z_{n,i} &:= \mathbb{E}[(\tilde{x}_{n,i})^2] = m_{n,i}(x_{n,i})^2 + (1 - m_{n,i})(v_i^2 + \sigma_i^2), \\ \eta_{n,i} &:= \text{Var}[\tilde{x}_{n,i}] = z_{n,i} - (y_{n,i})^2. \end{aligned}$$

2.3 M-Step. For the M-step, replacing \mathbf{x} with the virtual ensemble $\tilde{\mathbf{x}}$ requires computing the expectation with respect to $\tilde{x}_{n,i}$ of the mean and the covariance of each cluster. For simplicity, we henceforth focus on a “hard” EM algorithm in which each data point \mathbf{x}_n is fully assigned to a single cluster, although a “soft” version can be easily derived. We denote by \mathcal{C}_k the set of data point indices assigned to the cluster with index k . It is straightforward to show that

$$(\boldsymbol{\mu}_k)_i = \frac{1}{|\mathcal{C}_k|} \sum_{n \in \mathcal{C}_k} y_{n,i}, \quad (2.3)$$

$$(\boldsymbol{\Sigma}_k)_{ij} = \mathbb{E}[(\tilde{\boldsymbol{\Sigma}}_k)_{ij}] = \frac{1}{|\mathcal{C}_k|} \sum_{n \in \mathcal{C}_k} ((y_{n,i} - (\boldsymbol{\mu}_k)_i)(y_{n,j} - (\boldsymbol{\mu}_k)_j) + \eta_{n,i}\delta_{i,j}). \quad (2.4)$$

Note that this is the same formula as the classical M-step, but with $x_{n,i}$ replaced by the expected value $y_{n,i}$ of the virtual distribution \tilde{x} , plus a correction term to $\Sigma_{i,j}$ corresponding to the covariance matrix $\eta_{n,i}$ of \tilde{x} . Computation of these quantities can be carried out very efficiently as we can decompose $(\mu_k)_i$ and $(\Sigma_k)_{ij}$ as follows:

$$\begin{aligned}
 (\mu_k)_i &= \frac{1}{|\mathcal{C}_k|} \left(\sum_{n \in \mathcal{C}_k \setminus \mathcal{M}_{k,i}} y_{n,i} + |\mathcal{M}_{k,i}| v_i \right), \\
 (\Sigma_k)_{ij} &= \frac{1}{|\mathcal{C}_k|} \sum_{n \in \mathcal{C}_k \setminus (\mathcal{M}_{k,i} \cap \mathcal{M}_{k,j})} (y_{n,i} - (\mu_k)_i)(y_{n,j} - (\mu_k)_j) \\
 &\quad + \frac{|\mathcal{M}_{k,i} \cap \mathcal{M}_{k,j}|}{|\mathcal{C}_k|} (v_i - (\mu_k)_i)(v_j - (\mu_k)_j) \\
 &\quad + \frac{1}{|\mathcal{C}_k|} \left(\sum_{n \in \mathcal{C}_k \setminus \mathcal{M}_{k,i}} \eta_{n,i} + |\mathcal{M}_{k,i}| \sigma_i^2 \right) \delta_{i,j},
 \end{aligned} \tag{2.5}$$

where $\mathcal{M}_{k,i} = \{n \in \mathcal{C}_k | m_{n,i} = 0\} \subseteq \mathcal{C}_k$ denotes the set of points within cluster k for which feature i is fully masked. Note that if all data points in a cluster have feature i masked, then $(\mu_k)_i = v_i$, the noise mean, and $(\Sigma_k)_{ii} = \sigma_i^2$, the noise variance.

2.4 E-Step. In the E-step, we compute the responsibility of each cluster for each point, defined as the probability that point n came from cluster k , conditional on its feature values. The responsibility is computed via Bayes theorem from π_{nk} , the log likelihood of point n under the gaussian model for cluster k . In the masked EM algorithm, we compute π_{nk} as its expected value over the virtual distribution \tilde{x}_n . Thus, the algorithm acts as if each data point is replaced by an infinite ensemble of points drawn from the distribution of \tilde{x}_n , which must all be assigned the same cluster label. Explicitly,

$$\pi_{nk} = \mathbb{E}_{\tilde{x}_n} \left[-\frac{d}{2} \log 2\pi - \frac{1}{2} \log \det \Sigma_k - \frac{1}{2} (\tilde{x}_n - \mu_k)^T (\Sigma_k)^{-1} (\tilde{x}_n - \mu_k) \right]. \tag{2.6}$$

The final term of equation 2.6 corresponds to the expectation of the Mahalanobis distance of $\tilde{x}_{n,i}$ from cluster k . It can be shown that

$$\begin{aligned}
 \pi_{nk} &= -\frac{d}{2} \log 2\pi - \frac{1}{2} \log \det \Sigma_k - \frac{1}{2} (\mathbf{y}_n - (\mu_k))^T (\Sigma_k)^{-1} (\mathbf{y}_n - (\mu_k)) \\
 &\quad - \frac{1}{2} \left(\sum_i \eta_{n,i} (\Sigma_k)_{ii}^{-1} \right).
 \end{aligned}$$

This leads to the original E-step for the EM algorithm, but with $y_{n,i}$ substituted for $x_{n,i}$ plus a diagonal correction term $-\frac{1}{2} \sum_i \eta_{n,i} (\Sigma_k)_{ii}^{-1}$.

2.5 Penalties. Automatically determining the number of clusters in a mixture of gaussians requires a penalty function that penalizes overfitting by discouraging models with a large number of parameters. Commonly used penalization methods include the Akaike information criterion (AIC) (Akaike, 1974) and Bayes information criterion (BIC) (Schwarz, 1978):

$$\text{AIC} = 2\kappa - 2 \ln(L), \quad \text{BIC} = \kappa \ln(N) - 2 \ln(L),$$

where κ is the number of free parameters in the statistical model and L is the maximum of the likelihood for the estimated model and N is the number of data points.

For the classical mixture-of-gaussians fit, the number of parameters κ is equal to $K(\frac{p(p+1)}{2} + p + 1) - 1$, where K is the number of clusters and p is number of features. The elements of the first term in κ correspond to the number of free parameters in a $p \times p$ covariance matrix, a p -dimensional mean vector, and a single weight for each cluster. Finally, 1 is subtracted from the total because of the constraint that the weights must sum to 1 for a mixture model.

For masked data, the estimation of the number of parameters in the model is more subtle. Because masked features are replaced by a fixed distribution that does not vary between data points, the effective degrees of freedom per cluster are much smaller than $\frac{p(p+1)}{2} + p + 1$. We therefore define a cluster penalty for each cluster C that depends only on the average number of unmasked features corresponding to that cluster. Specifically, let $r_n := \sum_{j=1}^p m_{n,j}$ be the effective number of unmasked features for data point n (i.e., sum of the weights over the features). Define $F(r) := \frac{r(r+1)}{2} + r + 1$, where the three terms correspond to the number of free parameters in an $r \times r$ covariance matrix, mean vector of length r , and a mixture weight, respectively.

Our estimate of the effective number of parameters is thus

$$\hat{\kappa} = \sum_{k=1}^K \left(\frac{1}{|C_k|} \sum_{n=1}^{|C_k|} F(r_n) \right) - 1. \quad (2.7)$$

2.6 Implementation. The algorithm was implemented in custom C++ code, based on previously released open-source software for fast mixture-of-gaussians fitting termed KlustaKwik (Harris et al., 2000–2013). Because we require the algorithm to run in reasonable time on large numbers of high-dimensional data points, several approximations are made to give faster running times without significantly affecting performance. These include

not only hard classification but also a heuristic that eliminates the great majority of E-step iterations, a split-and-merge feature that changes the number of clusters dynamically if this increases the penalized likelihood, and an additional uniform distributed mixture component to catch outliers. The software can be downloaded from <https://github.com/klusta-team/klustakwik> (Harris, Kadir, & Goodman, 2013).

3 Evaluation

3.1 Mixture of Gaussians. We first demonstrate the efficacy of the masked EM algorithm using a simple data set synthesized from a high-dimensional mixture of gaussians. The data set consisted of 20,000 points in 1000 dimensions, drawn from seven separate clusters. The means were chosen by centering probability density functions of gamma distributions on certain chosen features. All covariance matrices were identical: a Toeplitz matrix with all the diagonal entries 1 and off-diagonal entries that decayed exponentially with distance from the diagonal. Figure 1A shows this data set in pseudocolor format.

Figure 1B shows a confusion matrix generated by the masked EM algorithm on this data, with the modified BIC penalty and masks defined by equation 2.1, indicating perfect performance. By contrast, Figure 1C shows the result of classical EM, in which many clusters have been erroneously merged; the results for AIC penalty are shown since using a BIC penalty yielded only a single cluster. To verify that this is not simply due to an inappropriate choice of penalty, we reran with the penalty term linearly scaled by various factors. Figure 1D shows the results of a penalty $0.5 \times$ AIC that gave more clusters than the ground-truth data. Even in this case, however, the clusters produced by classical EM contained points from a mixture of the original clusters and could not be corrected even by manual post hoc cluster merging. To systematically evaluate the effectiveness of both algorithms, we measured performance using the variation of information (VI) metric (Meilă, 2003), for which a value of 0 indicates a perfect clustering. Both algorithms were tested for a variety of different penalties measured in multiples of AIC (see Figures 1E and 1F). Whereas the masked EM algorithm was able to achieve a perfect clustering for a large range of penalties around BIC, the classical EM algorithm produced a poorer value of 1.83 (corresponding to the poor result of merging all the points into a single cluster).

Figure 2 shows how clustering performance depends on the precise choice of masking parameters α and β defined in equation 2.1, using BIC penalty. Good performance did not require a single precise parameter setting but could be obtained with a range of parameters with $\alpha \approx 2$ and $3 \leq \beta \leq 7$. The results illustrate the benefits of using a double-threshold approach in preference to a single threshold: performance when $\alpha = \beta$ is markedly worse than when $\beta > \alpha$.

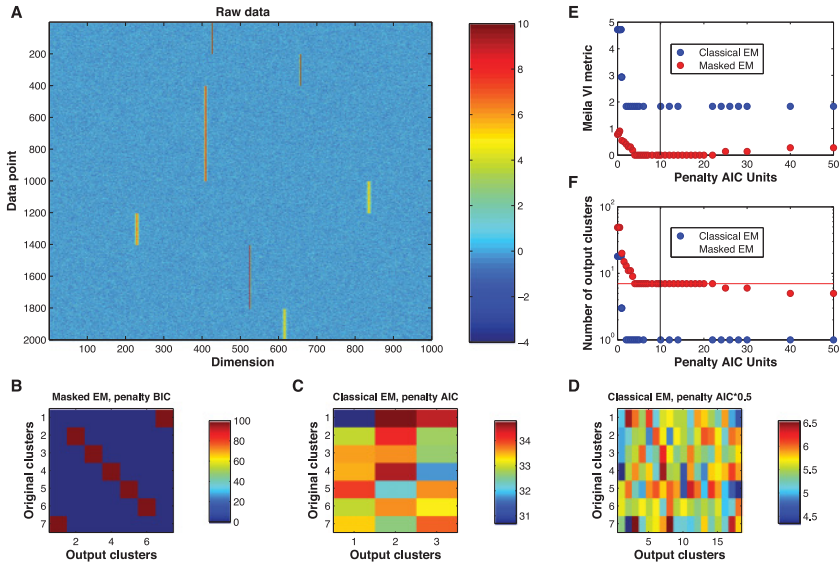


Figure 1: Simulated data. (A) Subsampled raw data. (B) Confusion matrix in percentages for masked EM with $\alpha = 2$, $\beta = 3$, and BIC penalty (equivalent to $10 \times$ AIC for 20,000 points). (C) Confusion matrix in percentages for classical EM for an AIC penalty. (D) Confusion matrix in percentages for classical EM for a penalty of $0.5 \times$ AIC. (E) VI metric measure of performance of both algorithms using various values for penalty, where the black vertical line indicates BIC. (F) The number of clusters obtained for various values of penalty, where the black vertical line indicates BIC.

Finally, in order to explore in more detail how the classical and masked EM algorithm deal with increasing dimensionality, we varied the number of features input to the algorithms. First, we sorted the features in rough order of relevance, according to the mean value of that feature over all input patterns. Both algorithms were then run on subsets of the most relevant p features for varying values of p . Performance was quantified with the VI metric (see Figure 3); in order to ensure differences between algorithms were not simply due to differences in penalty strategy, we also permitted post hoc manual merging of clusters that were overspilt. With fewer than 17 features, both algorithms performed badly. For 17 to 22 features, both algorithms perform perfectly; however, as more uninformative features were added, the performance of the classical, but not masked, EM algorithm started deteriorating. The performance of the masked algorithm remained good for all dimensionalities tested.

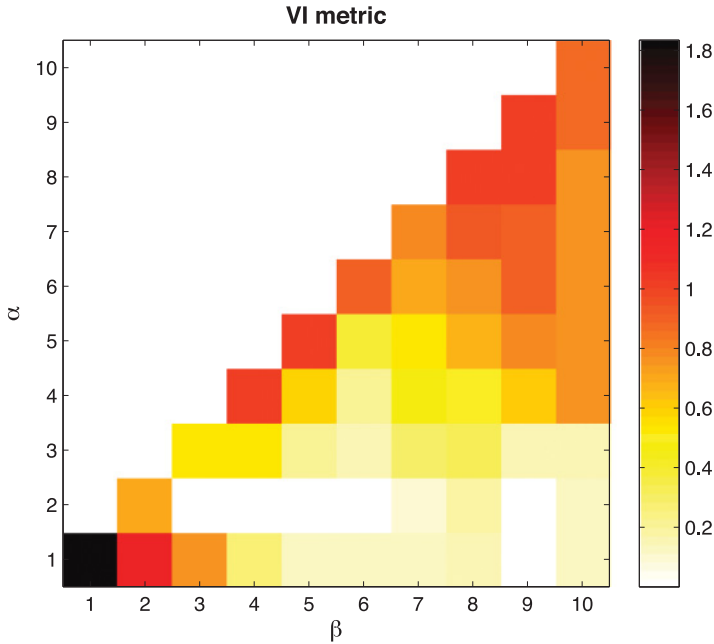


Figure 2: The effect of varying α and β in equation 2.1 for the simulated 1000-dimensional data set with seven clusters. The plot shows a pseudocolor representation of performance measured using the Meila VI metric for various values of α and β using BIC penalty.

3.2 Spike Sorting. To test the performance of the masked EM algorithm on our target application of high-channel-count spike sorting requires a ground-truth data set. Previous work established the performance of the classical EM algorithm for low-channel spike sorting with ground truth obtained by simultaneous recordings of a neuron using not only the extracellular array, but also an intracellular method using a glass pipette that unequivocally determined firing times (Harris et al., 2000). Because such dual recordings are not yet available for high-count electrodes, we created a simulated ground truth we term “hybrid data sets.” In this approach, the mean spike waveform on all channels of a single neuron taken from one recording (the donor) is digitally added onto a second recording (the acceptor) made with the same electrode in a different brain. Because the hybrid spikes are linearly added to the acceptor traces, this simulates the linear addition of neuronal electric fields and recreates many of the challenges of spike sorting, such as the variability of amplitudes and waveforms of the hybrid spike between channels, and overlap between the digitally added

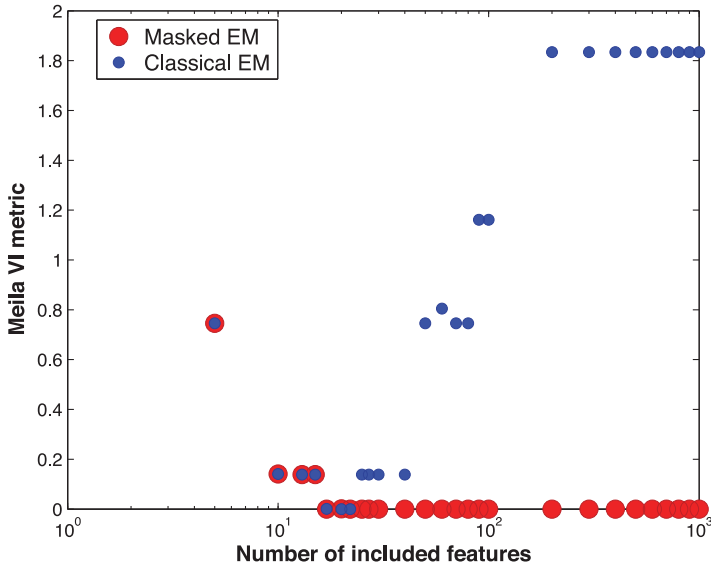


Figure 3: The effect of increasing the number of dimensions on the quality of cluster analysis. The dimensions are added in order of relevance relative to the seven ground-truth clusters of the simulated mixture of gaussians data set.

hybrid with spikes of other neurons in the acceptor data set (Harris et al., 2000). Furthermore, to simulate the common difficulty caused by of amplitude variability in bursting neurons, the amplitude of the hybrid spike was varied randomly between 50% and 100% of its original value. The hybrid data sets we consider were constructed from recordings in rat cortex kindly provided by Mariano Belluscio and György Buzsáki, using a 32-channel probe with a zig-zag arrangement of electrodes and minimum 20 μm spacing between neighboring contacts. Three principal components were taken from each channel, resulting in 96-dimensional feature vectors.

For the spike data, masks were generated using a generalization of equation 2.1 that took into account the topology of the electrode array. Data were first high-pass-filtered (500 Hz cutoff); then spikes were detected and masks were generated using a two-threshold flood-fill algorithm. The flood-fill algorithm finds spatiotemporally connected sets S of samples (t, c) (where t is time and c is channel number), for which the filtered signal exceeds a lower threshold α for every point in each set and each set contains at least one sample where the filtered signal exceeds an upper threshold β . The values of α and β were set as 2 and 4.5 times the standard deviation of the filtered signal, which was estimated robustly as a scaled median absolute deviation. For each spike, a mask for channel c was defined as

$\max_{t:(t,c) \in S} \theta(t, c)$, where $\theta(t, c) = \min(\frac{V(t,c) - \alpha}{\beta - \alpha}, 1)$. Spikes were resampled and aligned to a mean spike time estimated as $\bar{t} = \frac{\sum_{(t,c) \in S} t \theta_{t,c}}{\sum_{(t,c) \in S} \theta_{t,c}}$. Finally, feature vectors were extracted from the resampled filtered spike waveforms by principal component analysis channel by channel. For each channel, the first three principal components were used to create the feature vector; hence for a C -channel data set, each spike was given a $3C$ -dimensional feature vector. The component of the mask vector corresponding to each feature was obtained by taking as $\max_t \theta(t, c)$ computed on the channel from which the feature was derived. The data set contained 138,572 points of 96 dimensions; running 1500 iterations of the clustering algorithm on it took 10 hours on a single core of a 2.4 GHz Intel Xeon L5620 computer running Scientific Linux 5.5. (The data we analyzed are publicly available at https://github.com/klusta-team/hybrid_analysis.)

To evaluate the performance of the masked EM algorithm on this data set, we first identified the cluster with the highest number of true positive spikes and used it to compute a false discovery rate, $\frac{FP}{FP+TP}$, and a true positive rate, $\frac{TP}{FN+TP}$, where FP denotes the number of false-positive, TP the number of true-positive, and FN the number of false-negative spikes. This performance was compared against a theoretical upper bound obtained by supervised learning. The upper bound was obtained by using a quadratic support vector machine (SVM) (Cortes & Vapnik, 1995) trained using the ground-truth data, with performance evaluated by 20-fold cross-validation. In order to ensure we estimated maximal performance, the SVM was run over a large range of parameters such as margin and class weights, as well as including runs in which only features relevant to hybrid cells were included. The theoretical optimum performance was estimated as a receiver operating characteristic (ROC) curve by computing the convex hull of false discovery and true positive rates for all SVM runs.

Figure 4 shows the performance of the masked EM algorithm and classical EM algorithm on the hybrid data set, set against the theoretical optimum estimated by the SVM. While the masked EM algorithm performs at close to the estimated upper bound, the classical EM algorithm is much poorer. To verify that this poorer performance indeed resulted from a curse of dimensionality, we reran the classical EM algorithm on only the subset of features that were unmasked for the hybrid spike (9 out of 96 features). As expected, the upper-bound performance was poorer in this case, but the classical EM algorithm performed close to the theoretical upper bound. This indicates that the classical algorithm fails in high-dimensional settings, whereas the masked EM algorithm performs well.

4 Discussion and Conclusion

We have introduced a method for high-dimensional cluster analysis, applicable to the case where a small subset of the features is informative for

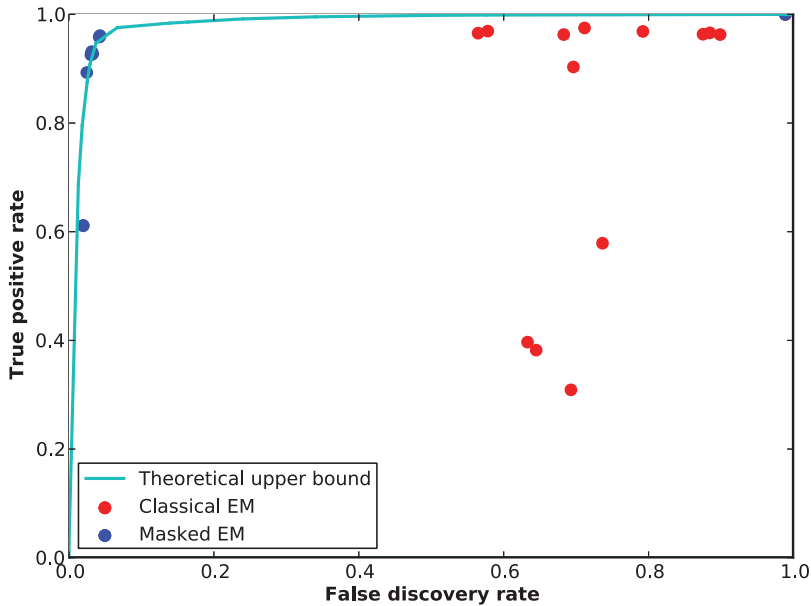


Figure 4: Performance of the masked and classical EM algorithms for a spike sorting data. Blue and red points indicate performance of multiple runs of the masked and classical EM algorithms with different penalty parameter settings. The cyan curve indicates optimal possible performance, estimated as the convex hull of supervised learning results obtained from a support vector machine with quadric kernel.

any data point. Unlike global feature selection methods, both the number and the precise set of unmasked features can vary between different data points. Both the number of free parameters and computational cost scale with the number of unmasked features per data point, rather than the total number of features. This approach was found to give good performance on simulated high-dimensional data and in our target application of neurophysiological spike sorting for large electrode arrays.

A potential caveat of allowing different features to define different clusters is the danger of artificial cluster splitting. If simply a hard threshold were used to decide whether a particular feature should be used for a particular cluster or data point, this could lead to a single cluster being erroneously split in two, according to whether the threshold was exceeded by noisy data. The masked EM algorithm overcomes this problem with two approaches. First, because the masks are not binary but real valued, crossing a threshold such as that in equation 2.1 leads to smooth rather than discontinuous changes in responsibilities; second, because masked features are replaced by a virtual distribution of empirically measured subthreshold data, the assignment of points with masked features is close to that

expected for the original subthreshold features. With these approaches in place, we found that erroneous cluster splitting was not a problem in simulation or in our target application.

In this study, we have applied the masking strategy to a single application of unsupervised classification using a hard EM algorithm for a mixture-of-gaussians fitting. However, the same approach may apply more generally whenever only a subset of features is informative for any data point and when the expectation of required quantities over the modeled subthreshold distribution can be analytically computed. Other domains in which this approach may work therefore include not only cluster analysis with soft EM algorithms or different probabilistic models but also model-based supervised classification.

References

- Akaike, H. (1974). A new look at the statistical model identification. *IEEE Transactions on Automatic Control*, 19(6), 716–723.
- Bouveyron, C., & Brunet-Saumard, C. (2012). Model-based clustering of high-dimensional data: A review. *Computational Statistics and Data Analysis*, 71, 52–78.
- Calabrese, A., & Paninski, L. (2011). Kalman filter mixture model for spike sorting of non-stationary data. *Journal of Neuroscience Methods*, 196(1), 159–169.
- Carin, L., Wu, Q., Carlson, D., Lian, W., Stoetzner, C., Kipke, D., . . . Dunson, D. (2013). Sorting electrophysiological data via dictionary learning and mixture modeling. *IEEE Transactions on Biomedical Engineering*, 61, 41–54.
- Cortes, C., & Vapnik, V. (1995). Support-vector networks. *Machine Learning*, 20(3), 273–297.
- Dempster, A. P., Laird, N. M., & Rubin, D. B. (1977). Maximum likelihood from incomplete data via the EM algorithm. *Journal of the Royal Statistical Society. Series B (Methodological)*, 39, 1–38.
- Einevoll, G. T., Franke, F., Hagen, E., Pouzat, C., & Harris, K. D. (2012). Towards reliable spike-train recordings from thousands of neurons with multielectrodes. *Current Opinion in Neurobiology*, 22(1), 11–17.
- Ekanadham, C., Tranchina, D., & Simoncelli, E. P. (2013). A unified framework and method for automatic neural spike identification. *Journal of Neuroscience Methods*, 22, 47–55.
- Fraley, C., & Raftery, A. E. (2002). Model-based clustering, discriminant analysis, and density estimation. *Journal of the American Statistical Association*, 97(458), 611–631.
- Franke, F., Natora, M., Boucsein, C., Munk, M. H. J., & Obermayer, K. (2010). An online spike detection and spike classification algorithm capable of instantaneous resolution of overlapping spikes. *Journal of Computational Neuroscience*, 29(1–2), 127–148.
- Friedman, J. H., & Meulman, J. J. (2004). Clustering objects on subsets of attributes (with discussion). *Journal of the Royal Statistical Society. Series B (Statistical Methodology)*, 66(4), 815–849.
- Gasthaus, J., Wood, F., Gorur, D., & Teh, Y. W. (2008). Dependent Dirichlet process spike sorting. In D. Koller, D. Schuurmans, Y. Bengio, & L. Bottou (Eds.), *Advances in neural information processing systems* (pp. 497–504). Cambridge, MA: MIT Press.

- Ghahramani, Z., & Hinton, G. E. (1996). *The EM algorithm for mixtures of factor analyzers* (Tech. Rep. CRG-TR-96-1). Toronto: University of Toronto.
- Harris, K. D., Henze, D. A., Csicsvari, J., Hirase, H., & Buzsáki, G. (2000). Accuracy of tetrode spike separation as determined by simultaneous intracellular and extracellular measurements. *Journal of Neurophysiology*, *84*(1), 401–414.
- Harris, K. D., Kadir, S. N., & Goodman, D. F. M. (2000–2013). *KlustaKwik*. <https://sourceforge.net/projects/klustakwik/files/>.
- Harris, K. D., Kadir, S. N., & Goodman, D. F. M. (2013). *Masked KlustaKwik*. <https://klusta-team.github.com/klustakwik>.
- Lewicki, M. S. (1998). A review of methods for spike sorting: the detection and classification of neural action potentials. *Network: Computation in Neural Systems*, *9*(4), R53–R78.
- Marre, O., Amodei, D., Deshmukh, N., Sadeghi, K., Soo, F., Holy, T. E., & Berry, M. J. (2012). Mapping a complete neural population in the retina. *Journal of Neuroscience*, *32*(43), 14859–14873.
- McLachlan, G. J., Peel, D., & Bean, R. W. (2003). Modelling high-dimensional data by mixtures of factor analyzers. *Computational Statistics and Data Analysis*, *41*(3), 379–388.
- Meilă, M. (2003). Comparing clusterings by the variation of information. In B. Schölkopf & M. K. Warmuth (Eds.), *Learning theory and kernel machines* (pp. 173–187). New York: Springer.
- Pillow, J. W., Shlens, J., Chichilnisky, E. J., & Simoncelli, E. P. (2013). A model-based spike sorting algorithm for removing correlation artifacts in multi-neuron recordings. *PLoS ONE*, *8*(5), e62123.
- Prentice, J. S., Homann, J., Simmons, K. D., Tkačik, G., Balasubramanian, V., & Nelson, P. C. (2011). Fast, scalable, Bayesian spike identification for multi-electrode arrays. *PLoS ONE*, *6*(7), e19884.
- Quian Quiroga, R., Nadasdy, Z., & Ben-Shaul, Y. (2004). Unsupervised spike detection and sorting with wavelets and superparamagnetic clustering. *Neural Computation*, *16*(8), 1661–1687.
- Raftery, A. E., & Dean, N. (2006). Variable selection for model-based clustering. *Journal of the American Statistical Association*, *101*(473), 168–178.
- Sahani, M. (1999). *Latent variable models for neural data analysis*. Doctoral dissertation, California Institute of Technology.
- Schwarz, G. (1978). Estimating the dimension of a model. *Annals of Statistics*, *6*(2), 461–464.
- Shoham, S., Fellows, M. R., & Normann, R. A. (2003). Robust, automatic spike sorting using mixtures of multivariate *t*-distributions. *Journal of Neuroscience Methods*, *127*(2), 111–122.
- Takahashi, S., Anzai, Y., & Sakurai, Y. (2003). Automatic sorting for multi-neuronal activity recorded with tetrodes in the presence of overlapping spikes. *Journal of Neurophysiology*, *89*(4), 2245–2258.
- Wood, F., & Black, M. J. (2008). A nonparametric Bayesian alternative to spike sorting. *Journal of Neuroscience Methods*, *173*(1), 1–12.